D. P. Landau K. K. Mon
H.-B. Schüttler (Eds.)

Computer Simulation Studies in Condensed Matter Physics III

Two-Dimensional Quantum Antiferromagnet at Low Temperatures

E. Manousakis

Department of Physics and Center for Materials Research and Technology,
Florida State University, Tallahassee, FL32306, USA

We discuss the spin-dynamics in the spin-$\frac{1}{2}$ antiferromagnetic Heisenberg model and the related quantum nonlinear σ model on the square-lattice at zero and low temperatures. We use mainly numerical methods, including variational Monte Carlo, quantum Monte Carlo and exact numerical diagonalization techniques. We compare our results to those obtained by other techniques and to certain experimental data obtained on undoped copper-oxygen antiferromagnetic insulators. Effects of hole-doping are briefly summarized in the framework of the strong-coupling Hubbard model.

1. Introduction

The Hubbard model in the large Coulomb-repulsion limit is under intensive theoretical study because it may be relevant to the physics behind the copper-oxide superconductors. Regardless of its connection to the high-temperature superconductors, the physics of a strongly-correlated electronic system should be understood at least in its simplest theoretical abstraction: the single-band Hubbard model. Low-order strong-coupling perturbation treatment of the Hubbard model produces an effective Hamiltonian[1] which operates in a restricted Hilbert space having states with no double-occupancy below half-filling. Ignoring a three-site interaction term this effective Hamiltonian is now known as the $t-J$ model

$$H_{t-J} = -t \sum_{<i,j>,\sigma} (c^{\dagger}_{i,\sigma} c_{j,\sigma} + h.c) + J \sum_{<i,j>} \left(S^z_i S^z_j + \frac{1}{2}(S^+_i S^-_j + S^-_i S^+_j) \right), \qquad (1.1)$$

where $S^z_i = \frac{1}{2}(c^{\dagger}_{i\uparrow} c_{i\uparrow} - c^{\dagger}_{i\downarrow} c_{i\downarrow})$, $S^+_i = c^{\dagger}_{i\uparrow} c_{i\downarrow}$ and $S^-_i = c^{\dagger}_{i\downarrow} c_{i\uparrow}$ and $c^{\dagger}$ is the fermion creation operator in the Hubbard model. This Hamiltonian is assumed to operate only in a subspace of the Hilbert space with states having no doubly occupied site. The $t-J$ model is interesting on its own and its derivation from the Hubbard model may serve as a motivation. At half-filling the hopping term of this Hamiltonian is inactive and thus (1.1) reduces to the spin-$\frac{1}{2}$ antiferromagnetic (AF) Heisenberg model (AFHM) on the square-lattice

$$H = J \sum_{<ij>} \vec{S}_i \cdot \vec{S}_j. \qquad (1.2)$$

The magnitude of the characteristic energy scale J of the model may be determined from the magnetic properties of the undoped materials. In two space dimensions (2D) the Heisenberg model cannot develop long-range-order (LRO) at any non-zero temperature[2]. Doubts expressed about the existence of LRO in the ground-state, because of the low-spin case and low-dimensionality of the model, are now more or less quenched. Even though there is no rigorous proof of the existence of AF LRO in the ground-state of the spin-$\frac{1}{2}$ 2D antiferromag-

Springer Proceedings in Physics, Vol. 53
Computer Simulation Studies in Condensed Matter Physics III

net[3], the picture of spin-wave theory[4] (SWT) has recently received significant support by several systematic approaches[5-10].

In the first part of this paper, we study the ground-state of (1.2) using the variational technique. We obtain[9,10] a variational wave function consistent with sum-rules for the dynamic structure function which gives accurate ground-state properties. Using this wave function, the sum-rules and the variational Monte Carlo (VMC) technique, we determine the spin-wave velocity, the spin-stiffness constant and staggered magnetization. The spin-wave velocity, the sublattice magnetization and the AF coupling J are accessible to experiments and this allows a direct test of the theory.

In section 3 of this paper we study the model (1.2) at finite temperatures using quantum Monte Carlo methods[11,12]. We also study the quantum nonlinear sigma model (QNLσM)[13] which is believed to be equivalent to the AFHM at low T[14]. The idea that models such as (1.1) may be relevant for the physics behind these materials is supported by the comparison of the temperature dependent spin-spin correlation length $\xi(T)$ obtained from these studies with that inferred by neutron scattering experiments[15]. We find that for the model (1.2), $\xi(T \rightarrow 0) = aexp(2\pi\rho_s/T)$, and the same form is valid for the QNLσM in the regime controlled by its ordered phase and at low T. One- and two-loop Renormalization Group calculations for the sigma model have been carried out by Chakravarty, Halperin and Nelson (CHN)[16,17]. Our results disagree with the results of their one-loop calculation[16] and are in agreement with their results obtained by calculating the β-function up to two-loop order[17]. Furthermore, our $\xi(T)$ agrees reasonably well with the neutron scattering data using $J = 1480K$. We conclude that SWT correctly describes the $T = 0$ properties of the spin-$\frac{1}{2}$ AFHM and the 2D thermal spin correlations in the model are consistent with those observed by neutron scattering.

Due to the fact that the Monte Carlo simulations of the model (1.1) are hindered by problems arising from the fermion statistics, the information about the phase diagram and superconductivity in the model is limited. In section 4 of this paper, we report certain results for the single-hole band obtained by VMC methods[18]. A wave function which takes into account spin-spin and spin-hole correlations is constructed following the ideas of Feynman-Cohen for the case of a helium-three atom moving in a background of liquid helium-four. Using this wave function and the VMC technique we calculate the hole excitation spectrum. For the case of two or more holes exact diagonalization studies[19] on small-size system indicate that there is a range of t/U where hole-pairing is possible.

2. Zero Temperature Properties

Antiferromagnets were initially treated using spin-wave theory[4] which assumes AF LRO in the ground-state and treats the zero-point motion of small quantum fluctuations about the classical Néel state perturbatively. This approach for a spin-S antiferromagnet is an expansion in powers of $1/(zS)$, z being the coordination number. The role of quantum fluctuations becomes more important for small S, and low-dimensional systems and it is natural to raise doubts about the convergence of this approach for the smallest possible spin case and for 2D spin-systems.

There is no rigorous proof of the existence or non-existence of AF LRO in the ground-state of (1.2) on the square-lattice for spin-$\frac{1}{2}$. However, a growing number of calculations[5-10] suggest that the picture obtained from SWT is correct. For example, using the Green's function Monte Carlo (GFMC) method, Carlson and independently Trivedi and Ceperley have performed accurate simulations[8] on up to 32×32 lattice size. They find that the ground-state energy per bond and staggered magnetization follows the finite-size scaling

expected from SWT. Their extrapolated values to the infinite lattice are $E_0/NJ = -0.6692 \pm 0.0002$ and $m^\dagger \simeq 0.31 \pm 0.01$. These results compare very well with those obtained from SWT[4], which are, respectively, 0.303 and -0.6704. Furthermore, they studied spin-wave states and concluded that the energy-gap scales as predicted by SWT and vanishes in the infinite-lattice limit.

In this section, we shall review certain results obtained with the variational approach. In Ref. 9, using a complete set of multi-magnon states, we calculated the matrix elements of the Hamiltonian (1.2) in a separability approximation originally developed for the treatment of strongly correlated quantum liquids. The ground-state wave function in this approximation is obtained as

$$|\psi_0 >= \exp\Big(-\frac{1}{2}\sum_{i<j} u_{ij}\sigma_i^z\sigma_j^z\Big)|\phi >, \tag{2.1.a}$$

$$u_{ij} \equiv \frac{1}{N}\sum_{\vec{k}}\Big(\sqrt{\frac{1+\gamma(k)}{1-\gamma(k)}} - 1\Big)e^{i\vec{k}.(\vec{R}_i - \vec{R}_j)}, \tag{2.1.b}$$

where $\gamma(\vec{k}) = 1/2(cos(k_x) + cos(k_y))$ and

$$|\phi >\equiv \frac{1}{\sqrt{2^N}}\sum_c (-1)^{L(c)}|c > . \tag{2.1.c}$$

The sum is over all possible spin configurations c of the lattice and $L(c)$ is the number of down spins in one sublattice contained in the configuration c. Therefore the state $|\phi >$ can be written as $|\phi >= \prod_{\vec{R}\epsilon A}|\vec{R}, + > \prod_{\vec{R}\epsilon B}|\vec{R}, - >$ and the states $|\vec{R}, + >$ and $|\vec{R}, - >$ are the eigenstates of $\hat{S}^x_{\vec{R}}$. A and B represent the two sublattices. Hence the state (2.1.c) has zero staggered magnetization in the z and y directions but has full staggered magnetization in the x direction. In fact, if we rotate the Néel state around the y-axis by $\pi/2$ we will obtain the state (2.1.c).

Variational wave functions of similar form have been studied earlier[20] by Hulthen and Kastelijn for one dimension and for one, two and three dimensions by Marshall and Bartkowski. More recently the same form was studied by Huse and Elser (HE) and by Horsch and Linden (HL) [21] using the VMC approach. HE took $u(1) = u_1$ and $u(r) = a/r^b$ for $r > 1$, where $r = |\vec{R}_i - \vec{R}_j|$ and treated u_1, a and b as variational parameters. The energy per site obtained in their calculation is $E_0/N \sim -0.664J$ for $u_1 \sim 0.65$, $a \sim 0.475$, and $b \sim 0.7$. HL used only $u(1)$ as a variational parameter (and $u(r > 1) = 0$) and they found $E_0/N \sim -0.644J$. Notice that our u is not a function of the distance r between two points on the lattice but rather a function of the two components x and y of the vector $\vec{R}_{ij}$. The form (2.1.b) has long-distance behavior consistent with the existence of long-wavelength spin-wave excitations. From Eq. (2.1.b) we find that

$$u(r \to \infty) = \frac{\sqrt{2}}{\pi r}. \tag{2.2}$$

The tails of the wave function of Ref. 21 and that of Eq. (2.2) are different. We have calculated the expectation value of the Heisenberg Hamiltonian (1.2) with the wave function (2.1) using MC integration and restricting the sum in $|\phi >$ (Eq. 2.1.c) over configurations having zero total S_z only. We found almost the same energy (slightly better (lower)) as that of HE. The advantage of the wave function (2.1) is its simple physical origin and the fact that it gives the same ground-state energy with no free parameter. Next, we improve the wave function (2.1) further using sum-rules of the dynamical structure function. We also propose a method to calculate the spin-wave velocity accurately.

We can use a representation in which the eigenstates of the spin-$\frac{1}{2}$ AFHM are expressed as a superposition of configurations $|c>$ labeled by the locations of one kind of spins (say the down spins) on the lattice, i.e., $|c>=|i_1, i_2, ...i_r>$. In this representation, we can show that the eigenvalue problem reduces to a difference equation identical to the many-particle Schrödinger equation on a 2D lattice (the "particles" correspond to down spins). In this quantum lattice-gas of bosons, the "particles" have "mass" $m = 2$ (in units of J and lattice-spacing a) and interact via a pair potential V_{ij} having an infinite on-site repulsion, $V_{ij} = 1$ if ij are n.n, otherwise $V_{ij} = 0$. This is a useful representation because our knowledge about the system of Bose-particles can be applied to the magnetic system also. For example, it is known that the ground-state of this system has a broken symmetry (condensate) which in the magnetic language corresponds to AF-LRO. The elementary excitations in the Bose-system are density fluctuations (phonons in the long-wavelength limit) which in the magnetic system correspond to spin-waves. Reatto and Chester have shown[22] that the zero-point motion of the long-wavelength modes of the Bose-system (zero-sound) gives rise to a long-range tail in the Jastrow wave function. For a 2D system, we obtain

$$u(r \to \infty) = \frac{mc}{4\rho_0 \pi r}, \tag{2.3}$$

where c is the spin-wave velocity. The ground-state of the Heisenberg antiferromagnet has zero total S_z and the number of down spins is exactly half the total number of sites giving $\rho_0 = 1/2$. Comparing the tails (2.2) and (2.3) we find $c = \sqrt{2}$ which is the value found by linear SWT.

We use[10] three ω-moments (sum rules) of the spin-dynamical structure function $S(\vec{q}, \omega)$ to determine the spin-wave velocity, assuming that a single-magnon state exhausts them in the long-wavelength limit. Using the ω^0-moment (the static structure function $S(\vec{q}) \equiv \langle 0|S^z_{-q} S^z_q|0\rangle$) and ω^1-moment we obtain

$$c = \frac{f}{s_1}, \tag{2.4.a}$$

where s_1 is the slope of $S(\vec{q})$ and

$$f \equiv -\frac{J}{4} \sum_{\delta} \langle 0|(S^+_i S^-_{i+\delta} + S^-_i S^+_{i+\delta})|0\rangle. \tag{2.4.b}$$

The value of c calculated from (2.4) is sensitive to both the tail of the wave function and finite-size effects. As in the case of quantum liquids we shall use a different and more accurate way to determine c, explained next.

We have obtained a third sum rule analogous to the compressibility sum rule in the case of quantum fluids which in the spin-system is translated to "magnetic susceptibility sum-rule" (ω^{-1} moment). Again assuming that this sum-rule in the long-wavelength limit is exhausted by a single-magnon-excitation we obtain

$$c = \sqrt{2f\epsilon''}. \tag{2.5}$$

Here ϵ'' is the second derivative of the energy per particle $\epsilon(M)$ with respect to the magnetization density $M = 1/N < \sum_i S^z_i >$. We note that the magnetization density corresponds to the particle density in the Bose system and the energy $\epsilon(M)$ to the ground-state equation of state. We calculate ϵ'' by restricting ourselves to a subspace with well-defined $S^z_{tot} = M$, i.e., total z-component of the magnetization. Therefore, we can determine the spin-wave velocity in a way analogous to that used in the case of quantum liquids to calculate the

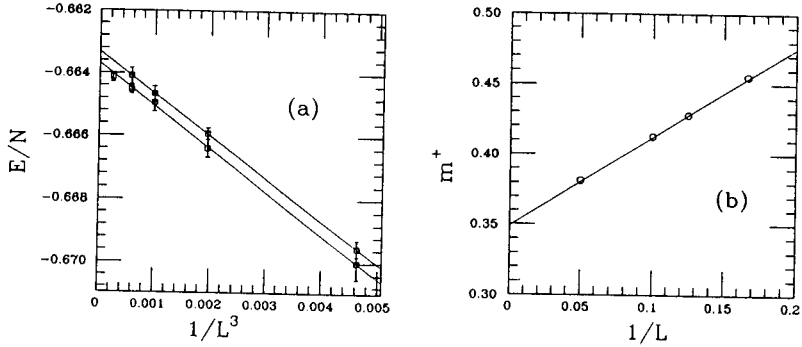

Figure 1. a) The energy per site as a function of L^{-3} for an L^2 lattice. The results are obtained with the parameter-free wave function (2.1) (upper line) and with the improved wave function (lower line). b) The staggered magnetization versus L^{-1} with the improved wave function.

sound velocity. This technique is known to be accurate for numerical studies, because it is not too sensitive to finite-size effects and to the tail of the ground-state wave function.

In the variational calculation we used the form (2.1.a), including in the sum (2.1.c) only states with zero magnetization, and took $u(1)$ and $u(\sqrt{2})$ as variational parameters and

$$u(\vec{r}) = \alpha u_0(\vec{r}), \quad for \quad \sqrt{x^2+y^2} \geq 2, \tag{2.6}$$

where $u_0(\vec{r})$ is that given by Eq. (2.1.b) and α is a parameter of order 1. We did not treat α as a variational parameter because the ground-state energy is not too sensitive to its precise value. Instead it is determined self-consistently by satisfying the third sum-rule (2.5). Given a value of α, we perform the variational calculation and determine $\epsilon(M)$ and the spin-wave velocity c from the slope of $\epsilon(M)$ via (2.5). Using the Chester and Reatto [22] relation (2.3), we obtain a new value of α from the relation $\alpha = c/\sqrt{2}$. This can be iterated until the input and the output value of α are the same. This procedure converges very quickly since as mentioned the energy $\epsilon(M)$ is not sensitive to the α. Starting from $\alpha = 1$ the output value of α obtained from $\epsilon(M)$ is ~ 1.2. In the next step using the new value of α as input we obtain practically the same output value from $\epsilon(M)$.

The calculation is performed on lattices of several sizes up to 20^2. In Fig. 1.a we present the ground-state energy per site as function of L^{-3} [23,7] for lattices of size $N = L^2$. The energy obtained with the wave function (2.1.c) (upper line) and with the improved wave function (2.6) (lower line) are the same within error bars. The advantage of the improved wave function, however, is that it is consistent with the sum rules and gives a more accurate excitation spectrum. The extrapolated value of the energy upper bound to the infinite-size lattice is $-0.6637J \pm 0.0002$, while the best estimate for the exact value obtained by GFMC calculations[8] is $-0.6692J \pm 0.0001$. Fig. 1.b shows the square root of the expectation value of the square of the staggered magnetization $m^\dagger$ obtained with the improved wave function. We obtain $m^\dagger = 0.349 \pm 0.002$ for the infinite lattice. This is close to the values of 0.34 ± 0.01 and 0.31 ± 0.01 reported in Ref. 8, while their guiding trial functions give somewhat higher value of $m^\dagger$ than ours. In Fig. 2, we give $\epsilon(M)$ versus M^2 for several lattice-sizes. Notice that ϵ'' is independent of the lattice-size within error bars and we obtain $\alpha = 1.22 \pm 0.02$. The value of this parameter (commonly called Z_c) is in good agreement with the value 1.158 obtained by spin-wave theory[4] and that obtained by GFMC [8] calculations and series expansions [24]. The same value of ϵ'' is required to fit at small M the exact diagonalization results for a 4×4 size lattice which have been obtained with methods explained in Ref. 19.

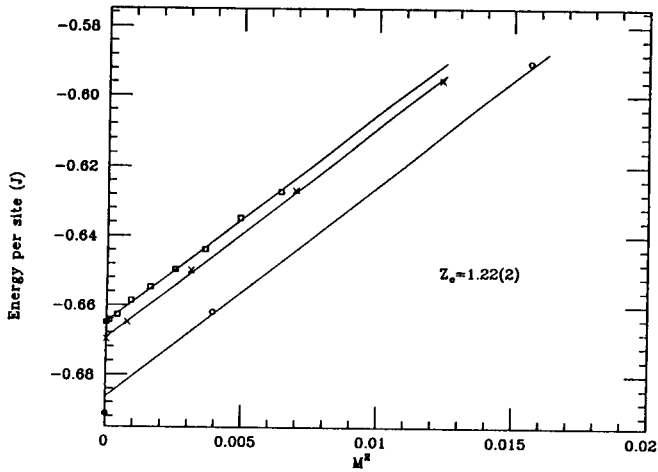

Figure 2. The energy per site as a function of the square of the total magnetization M^2 for 4×4, 6×6, and 10×10 lattices. The slope is related to the spin-wave velocity via Eq. 2.5.

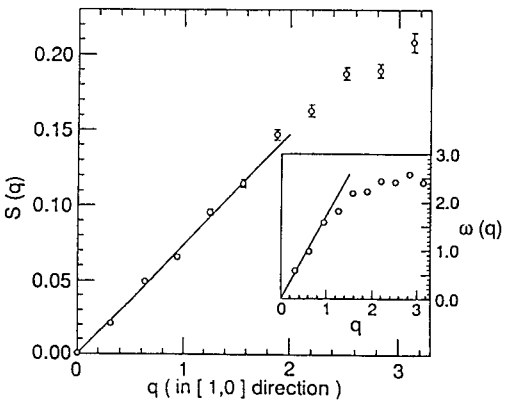

Figure 3. $S(\vec{q})$ calculated with the wave function (2.6) with $\alpha = 1.22$. The straight line has a slope $s_1 = f/c$. The inset is the calculated $\omega(\vec{q})$. The straight line in the inset has a slope equal to $c = 1.22\sqrt{2}$ as obtained from (2.5)

Hence, we expect the error in the calculation of c due to the approximate nature of our wave function to be small.

In Fig. 3, we give the calculated $S(\vec{q})$ using $\alpha = 1.22$ in the wave function. The straight line has a slope $s_1 = f/c$. The inset is the $\omega(\vec{q})$ calculated assuming that a single-magnon excitation exhausts the ω^0 and ω^1 sum-rules. The straight line in the inset has a slope $c = 1.22\sqrt{2}$. Hence the spin-wave spectrum in the long-wavelength limit, although noisy as expected, is consistent with this sum-rule within error bars also. In our units $Z_\chi = 8\chi J = 8J/\epsilon'' = 0.667 \pm 0.004$, which is higher than the spin-wave value of 0.449 and close to that reported in Ref. 25.

3. Low Temperature Properties. Nonlinear σ Model

Using Handscomb's quantum Monte Carlo method we have simulated[11] the spin-$\frac{1}{2}$ AFHM on the square lattice at finite temperatures. From the spin-spin correlation function we extracted the correlation length $\xi(T)$. We found that $\xi(T)$ increases very rapidly with decreasing temperature. In our first paper[11] we attempted to fit the temperature dependence of $\xi(T)$ to the form

$$\xi(T \to 0) = \frac{a}{T} exp\Big(\frac{2\pi\rho_s}{T}\Big), \tag{3.1}$$

as suggested by spin-wave theory. We concluded that our numerical results are inconsistent with this form. We also attempted to fit our results to a Kosterlitz-Thouless form and obtained a good quality fit. In Fig. 4.a we reproduce our Fig. 3 from Ref. 11 for easy reference. The dashed-dotted line was our best fit of the numerical results (points with the error bars for various size lattices as indicated on the figure) to the form (3.1), while the solid line was the fit to the Kosterlitz-Thouless form. The dashed-line is our results of the leading contribution at high temperatures [12]. We suggested that either (a) the form (3.1) is incorrect or valid at lower temperatures inaccessible to our simulation technique or (b) topological excitations may play an important role in the thermodynamics of (1.2). The form (3.1) is also obtained by Chakravarty, Halperin and Nelson (CHN)[16], studying the equivalent QNLσM by Renormalization Group with the β-function calculated with weak-coupling perturbation theory up to one-loop order and by the Schwinger-boson mean field calculations of Arovas and Auerbach and by the modified spin-wave theory by Takahashi at finite temperatures[26].

The improved two-loop calculation of CHN [17], however, shows that the prefactor in (3.1) is different, namely the correlation length at low T behaves as

$$\xi(T \to 0) = C_\xi exp\Big(\frac{2\pi\rho_s}{T}\Big). \tag{3.2}$$

Hence, CHN [17] point out that higher-order corrections are important and one should expect a constant prefactor. In Fig. 4.b we plot $T ln\xi(T)$ versus T/J to demonstrate that (3.2) is a very good approximation to the Monte Carlo results of Ref. 11. The fit gives $\rho_s \simeq 0.22J$ and $C_\xi = 0.25$. This value of ρ_s is in good agreement with the value found in section 2 by studying the ground-state of (1.2). On the basis of our results given in the

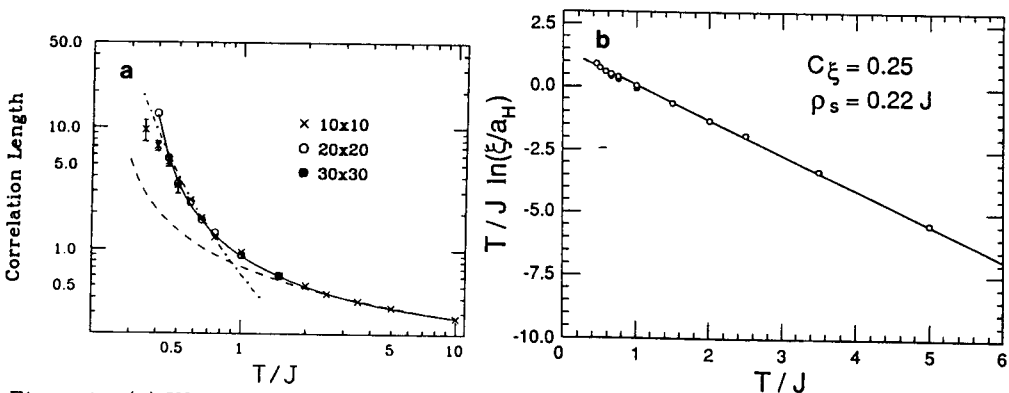

Figure 4. (a) We reproduce our Fig. 3 from Ref. 11 for easy reference. See text for explanations. (b) We plot the same data as $T ln\xi(T)$ versus T/J to demonstrate that (3.2) is a very good approximation.

previous section, the results of this fit to the temperature dependence of ξ and the results of our calculation of the σ model explained next, we conclude that, even though a Kosterlitz-Thouless phase cannot be theoretically excluded, there is no need to invoke the presence of such transition. Furthermore, our calculations[11,12,13] strongly support the results of the two-loop calculation of CHN [17] and the form (3.2) at low T.

Next, we briefly outline the results obtained[13] on the quantum non-linear σ model using both MC simulation and saddle point approximation. We shall show that the spin-$\frac{1}{2}$ AFHM corresponds to the ordered phase of the σ model where $\xi(T)$ obtained from the σ model in that phase agrees with the form (3.2).

The action for the nonlinear σ model in two-space one-Euclidean time dimensions is defined as[14]

$$S_\sigma = \frac{\rho_\sigma}{2\hbar c_\sigma} \int_0^{\beta\hbar c_\sigma} d\tau \int dx dy \Big((\partial_x \vec{n})^2 + (\partial_y \vec{n})^2 + (\partial_\tau \vec{n})^2 \Big). \tag{3.3}$$

Here $\vec{n}$ is a three-component vector field living on a unit sphere, c is the spin-wave velocity and $\beta = 1/K_B T$. It is known that the model (3.3) can be derived[14] from the model (1.2) in the long-wavelength limit. The Euclidean-time is a result of the quantum nature of the problem, and is introduced via the Trotter-Suzuki formula in the calculation of the trace of $exp(-\beta \hat{H})$, when the operator (1.2) is used. The Heisenberg antiferromagnet maps[14] onto this same model for arbitrary spin in 2D, the different values of S corresponding to different values of ρ_s and c_σ. The field $\vec{n}(\vec{x})$ is proportional to the average staggered magnetization in the model (1.2). We discretize the space-time and put the model on the 2+1 dimensional lattice:

$$S_\sigma = -\frac{1}{2g} \sum_{\vec{x}} \sum_{\mu=1}^{3} \vec{n}_l(\vec{x}).\Big(\vec{n}_l(\vec{x} + \hat{e}_\mu) + \vec{n}_l(\vec{x} - \hat{e}_\mu) \Big), \tag{3.4}$$

where $g = \hbar c_\sigma / \rho_\sigma a$ and $\vec{x}$ covers the 2+1 dimensional lattice of lattice spacing a, size $L^2 L_\beta$ and

$$\beta \hbar c_\sigma = L_\beta a. \tag{3.5}$$

Let us first study the $T = 0$ case. In this case we consider $L_\beta = L \to \infty$ and the theory has only one parameter, the dimensionless parameter g. We have calculated the staggered magnetization expectation value defined as $\bar{n}_l = < \left(\frac{1}{L^3} \sum_{x_\mu} \vec{n}_l(x_\mu) \right)^2 >$, where the expectation value is taken with respect to the distribution $exp[-S_\sigma(\{\vec{n}_l(x_\mu)\})]$. We expect the ground-state staggered magnetization to obey the finite-size scaling similar to that of Fig. 1.b for $m^\dagger$[23,7]. The extrapolated values $n_0(g) \equiv \bar{n}_l(g, L \to \infty)$ are shown in Fig. 5. Assuming that the spin-S quantum AFHM is equivalent to the QNLσM, the parameter g corresponds to the different possible spin values. There is a value of g that gives the same staggered magnetization as extracted from the quantum spin-$\frac{1}{2}$ AFHM. In section 2 we found that the expectation value of the staggered magnetization is about 0.60 ± 0.02 its classical value. From Fig. 5, we find that at $g = 1.125$ the σ model gives the same staggered magnetization.

We calculated the β-function with a finite-size scaling technique by holding one lattice-dimension (say the Euclidean-time dimension) finite. We shall take the limit $L \to \infty$ and keep the time dimension finite so that Eq. (3.5) is satisfied. If, therefore, L is large enough so that $\xi_l << L$, the correlation length is only a function of L_β and g and in physical units is given by

$$\xi = \xi_l(g, L_\beta) a. \tag{3.6}$$

Substituting a from (3.5) in (3.6) we obtain

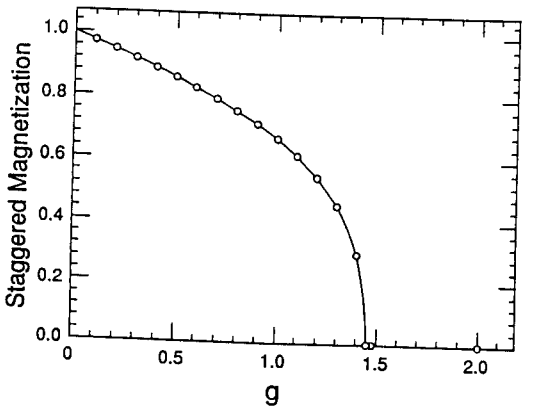

Figure 5. The extrapolated values $n_0(g) \equiv \bar{n}_l(g, L \to \infty)$.

$$\frac{\xi}{\beta \hbar c_\sigma} = \frac{\xi_l(g, L_\beta)}{L_\beta}. \tag{3.7}$$

At this point we wish to approach the continuum limit and hold the correlation length ξ fixed in units of the length-scale $\hbar c_\sigma \beta$, while $L_\beta \to \infty$. Clearly this can be done provided that a value of $g = g_c$ exists at which $\xi_l(g_c, L_\beta \to \infty) \to \infty$ in such a way that the ratio

$$b = \frac{\xi_l(g, L_\beta)}{L_\beta} \tag{3.8}$$

remains constant. A similar discussion in the framework of finite-size scaling at the phase transition can be found in a paper by Brèzin[27]. The critical point $g = g_c$ is a fixed point of the scale transformation $L_\beta \to L'_\beta$ and $g \to g'$ defined as follows:

$$\frac{\xi_l(g, L_\beta)}{L_\beta} = \frac{\xi_l(g', L'_\beta)}{L'_\beta}. \tag{3.9}$$

For large L_β this equation defines $g(L_\beta)$, which via (3.9) gives the function $g(a)$. In Fig. 6, b is given as a function of g calculated at $L_\beta = 2, 4, 8$ (for large enough space extent L so that finite-size effects on ξ_l due to finite L are negligible). We clearly see the presence of a critical point at $g_c \simeq 1.45$. Compare this value of g_c and the value of g_c where $n_0(g)$ vanishes in Fig. 5. The β function (and $a(g)$) determined via (3.9) close to the critical point is given by

$$\beta(g) = -\beta_1(g - g_c) + \ldots \tag{3.10.a}$$

with $\beta_1 \simeq 1.3 \pm 0.1$. By integrating the equation $\beta(g) = -a\frac{dg(a)}{da}$ we obtain

$$a(g) = a_0 |g - g_c|^\nu \tag{3.10.b}$$

where $\nu = 1/\beta_1 \simeq 0.77 \pm 0.07$, while the textbook value for ν is ~ 0.7. The results do not depend strongly on the errors in the determination of the function $a(g)$, i.e., the precise value of ν. Here, using $\nu = 0.7$, we find essentially the same results as those obtained in Ref. 13.

Having approximately determined the function $a = a(g)$, we can proceed to study the behavior of the correlation at low T. Using Eq. (3.5) and $a(g)$ we find that

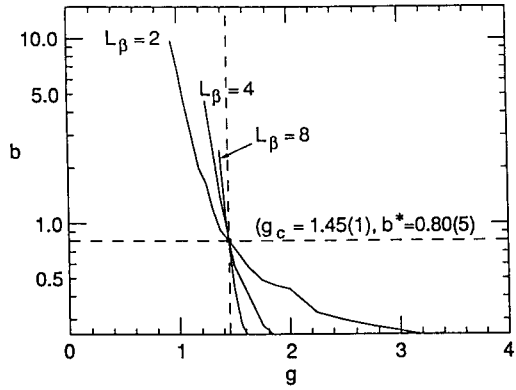

Figure 6. The ratio $b = \xi_{\rm latt}/L_\beta$ versus g for different L_β. Notice that all the lines for different L_β pass through the same point (g_c, b^*).

$$t \equiv \frac{T}{T_0} = \frac{1}{L_\beta |g - g_c|^\nu}, \tag{3.11.a}$$

where the constant temperature scale T_0 is defined as

$$k_B T_0 \equiv \frac{\hbar c_\sigma}{a_0}. \tag{3.11.b}$$

Furthermore, substituting (3.10.b) in (3.6) we obtain

$$\xi_0 \equiv \frac{\xi}{a_0} = \xi_l(g, L_\beta)|g - g_c|^\nu. \tag{3.11.c}$$

Namely, given the value of the correlation length $\xi_l(g, L_\beta)$ for given values of g and L_β, using the Eqs (3.11) we can calculate the physical correlation length in units of the constant length-scale a_0 and the physical temperature in units of the constant temperature-scale T_0 defined by (3.11.b). Using the calculated correlation lengths for various values of g and L_β we calculate ξ_0 and the corresponding t (using (3.11.a) and (3.11.c)) and plot them to obtain a single curve $\xi_0(t)$, shown in Fig. 7.a .

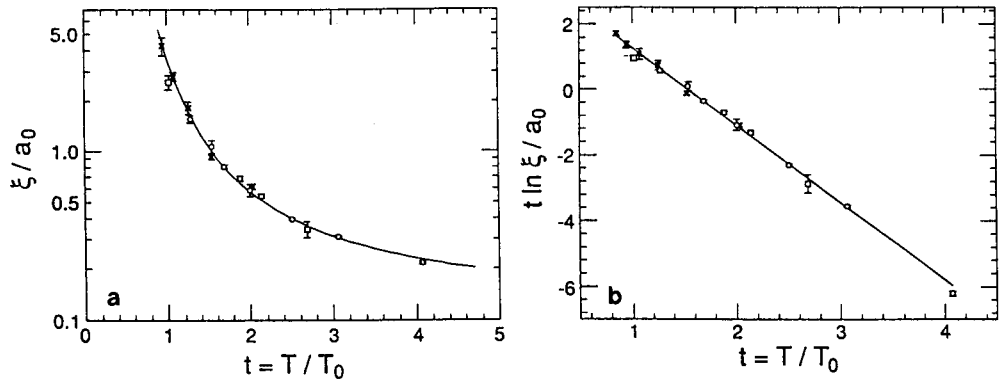

Figure 7. (a) The function $\xi_0(t)$ (see text for definition). Our data for various g's collapse on the same curve by using the calculated renormalization group β-function. The solid line corresponds to an exponential fit. (b) Demonstration that the correlation length as a function of T can be approximated by $ae^{b/T}$.

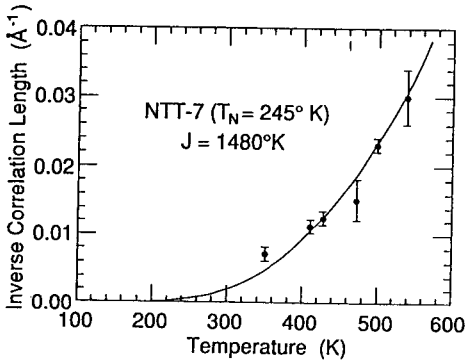

Figure 8. The solid line corresponds to an exponential fit to both our results for the nonlinear σ model and the spin-$\frac{1}{2}$ AFHM. We used the value $J = 1480K$ for the AF coupling. The solid circles with error bars are neutron scattering data taken on the insulator La_2CuO_4.

The fact that $\xi(T)$ obeys the expression obtained by the two-loop calculation of CHN, i.e., Eq. (3.2), is demonstrated in Fig. 7.b where the function $tln(\xi_0(t))$ can be approximated by a straight line. A straight-line fit gives

$$\xi/a_0 = Aexp\Big(B\frac{T_0}{T}\Big) \tag{3.12}$$

with $A = 0.093 \pm 0.002$ and $B = 3.64 \pm 0.02$. The constants a_0 and T_0 cannot be determined within the non-linear σ model since there are two parameters in the model, namely g and c_σ. Assuming that the σ model describes the continuum limit of the $S = 1/2$ AFHM, we can determine a_0 and T_0 in terms of J and the lattice spacing a_H of the lattice in which the spins in the Heisenberg model reside. Comparing (3.12) with (3.2) obtained from the AFHM, with $\rho_s = 0.227J$ and $C_\xi = 0.25a_H$, we find $a_0 = 2.69a_H$ and $T_0 = 0.392J$. Using the expression (3.11.b) we find $\hbar c_\sigma = 1.05Ja_H$. c_σ is a parameter of the σ model, not the physical spin-wave velocity.

The inverse correlation length versus T as observed by neutron scattering experiments[15] done on the undoped La_2CuO_4, is compared with our results in Fig. 8. The solid curve is the exponential given by Eq. (3.2) which fits the results for $\xi(T)$ obtained from the nonlinear σ model and AFHM. In the plot we used $a_H = 3.8\mathring{A}$, the $Cu - Cu$ distance, and $J = 1480K$. This value of J is close to the value reported by Raman scattering experiments[28]. Using this value of J and the expression $c = 1.22\sqrt{2}Ja$ we obtain $c \simeq 0.84eV - \mathring{A}$, a value higher than the lower bound of $0.6eV\mathring{A}$ reported by thermal neutron scattering studies[15] and closer to the more recent value of $0.85eV\mathring{A}$ inferred from high-energy inelastic neutron scattering[29].

4. Hole Dynamics

Following the mapping of the spin-$\frac{1}{2}$ AFHM to the quantum lattice-gas model of bosons, the problem of a hole in a quantum antiferromagnet (in the framework of the $t - J$ model) can be mapped to an impurity moving in a Bose system. Feynman and Cohen[30] have proposed a variational wave function for the motion of a ^3He impurity in liquid ^4He. This wave function takes into account the background boson-boson short-range correlation due to the hard core interaction and impurity-boson backflow correlations. We have studied [18] the following variational wave function which includes spin-spin and spin-hole ("spin-backflow") correlations

$$|\Psi(\vec{k})>=\frac{1}{\sqrt{N}}\sum_{\vec{R}}e^{-i\vec{k}\cdot\vec{R}}\hat{G}_{\vec{k}}|\phi(\vec{R})> \tag{4.1}$$

where $|\phi(\vec{R})>$ is the state (2.1.c) with a hole at $\vec{R}$. The correlation operator $\hat{G}_{\vec{k}}$ has the following form:

$$\hat{G}_{\vec{k}}=exp\Big(\sum_{\vec{r}}\Big(ig_{\vec{k}}(\vec{r})+h_{\vec{k}}(\vec{r})\Big)S^z_{\vec{R}+\vec{r}}-\frac{1}{2}\sum_{i<j}u(r_{ij})S^z_iS^z_j\Big). \tag{4.2}$$

The second term keeps the bosons from coming close to each other and from facing the hard core. The real function $h_{\vec{k}}(\vec{r})$ takes into account the hole-spin short-range correlations, while the term $ig_{\vec{k}}(\vec{r})$ represents the change in the phase of the wave function of the impurity in order to conserve local current in its motion.

Such backflow correlations in the case of a ^3He impurity in liquid ^4He are responsible for the large effective mass of the impurity. In the magnetic language the origin of the second term is the same as that in the pure AFHM and creates spin-fluctuations (the $|\phi>$ state is a Néel state in the x-direction therefore the $S^z_iS^z_j$ term creates pair-fluctuations). The first term couples the almost Néel state with the state where the hole hops to a neighboring site. In general u_{ij} may depend on the distance from the hole. In practice we find no significant lowering of the hole energy by allowing for such a non-uniform u_{ij}. Therefore, we used the same u_{ij} as that found in the VMC calculation at half-filling (AFHM) which is explained in section 2. Using the Metropolis algorithm we calculated[18] the expectation value of the $t-J$ Hamiltonian with the wave function (4.1-2) for one hole.

Fig. 9.a compares our variational results for the energy of a hole (we have subtracted the energy of the no-hole state) moving with $\vec{k}=(\frac{\pi}{2},\frac{\pi}{2})$ for the two cases, $g_{\vec{k}}=0$, and for the optimal value of $g_{\vec{k}}$, with exact diagonalization results on the 4×4 lattice [31] for several values of J/t. The introduction of the spin-hole correlations ($g_{\vec{k}}\neq0$) improves the energy significantly. The variational wave function is reasonably good for $J>t$; for lower values of J/t we need to improve the wave function with the inclusion of three-body correlations. Similar results are found for the 10×10 lattice.

The single-hole energy $e(\vec{k})$ as a function of the momentum $\vec{k}$ is calculated for several values of J/t. A typical result is shown in Fig. 9.b calculated for $J/t=1$ on a 10×10

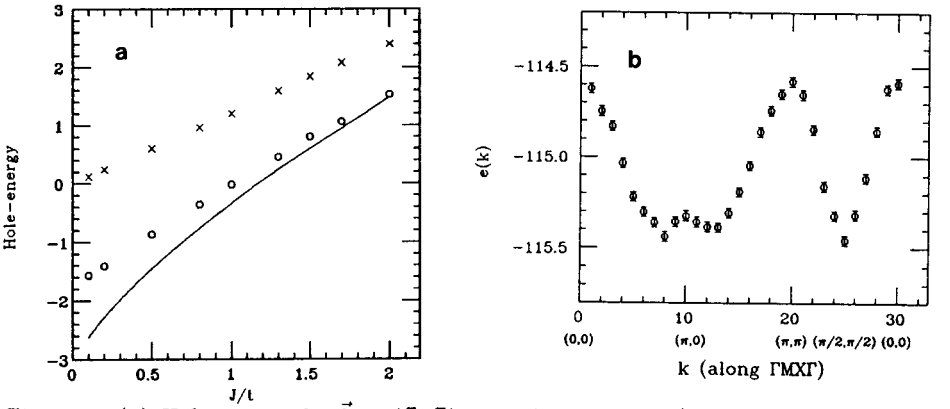

Figure 9. (a) Hole energy for $\vec{k}=(\frac{\pi}{2},\frac{\pi}{2})$ as a function of J/t. The solid line is exact diagonalization results[31], while the crosses and circles are

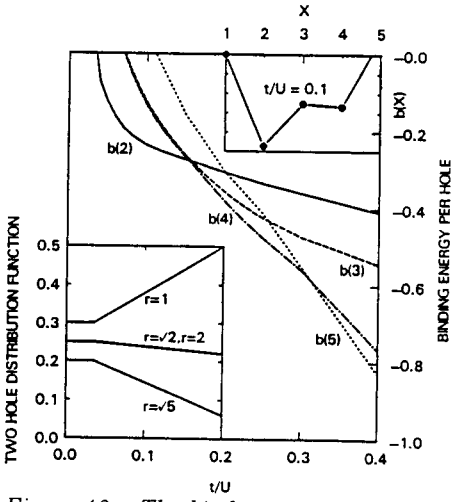

Figure 10. The binding energies per hole $b(X)$ for a system of X holes as a function of t/U. The lower-left inset gives the hole-hole distribution function for various distances. The top-right inset demonstrates the "magic" numbers for even number of holes.

lattice. We have not subtracted the no-hole energy in this case. The curve has a minimum at $\vec{k} = (\frac{\pi}{2}, \frac{\pi}{2})$. The maximum value is at $\vec{k} = (0,0)$ or $\vec{k} = (\pi, \pi)$ and both values are the same within error bars. The bandwidth decreases with J/t. We also find, in agreement with other authors[31,32], that the effective mass of the hole in the direction towards $(0, \pi)$ is larger than that in the direction towards $(0,0)$.

We have also calculated[18] the spin-hole-spin correlation function with one of the spins staying far away and the other close to the hole, using the variational wave function (4.1-2). In the static-hole case (t=0), we find that the staggered magnetization is enhanced in the neighborhood of the hole in accord with the results of Ref. 33. In the mobile-hole case (for $t/J \sim 1$), however, the staggered magnetization near the hole is significantly reduced from its bulk value in agreement with the spin-bag model of Schrieffer et al.[34].

Next, we shall discuss results obtained by exact diagonalization studies of the strong-coupling Hubbard Hamiltonian [19] on finite clusters of 10-sites. This Hamiltonian, in addition to the terms present in the $t - J$ model (1.1), involves a three-site hopping term. The full Hamiltonian is given in Ref. 19. First, it is also found that the minimum of the band in the AF phase is at $(3\pi/5, \pi/5)$, which is the closest wave vector to $(\pi/2, \pi/2)$ from the the 10 possible $\vec{k}$-vectors.

In Fig. 10 we plot the binding energy per hole obtained in Ref. 19 and defined as

$$b(X) = \frac{E(X) - XE(1)}{X} \tag{4.3}$$

where $E(X)$ is the total energy of the system containing X holes, measured from the energy of the no-hole state. Notice that there is a range of t/U $(0.04 < t/U < 0.16)$ where two-hole pairing is favored against multi-hole clustering or phase separation. At larger values of t/U multi-hole clustering is possible as can been seen in the figure (see also Ref. 19). The lower left inset shows the hole-hole distribution function and the top-right inset shows $B(X)$ versus X. The latter inset demonstrates that the peaks in $b(X)$ occur at even hole numbers.

5. Acknowledgements

This work was supported in part by the Florida State University Supercomputer Computations Research Institute which partially funded by the U.S. Department of Energy under Contract No. DE-FC05-85ER25000 and in part by the DARPA sponsored Florida Initiative in Advanced Microelectronics and Materials under Contract No. MDA972-88-J-1006.

6. References

1. J.E. Hirsch, Phys. Rev. Lett. **54**, 1317 (1985). K. Huang and E. Manousakis, Phys. Rev. **B36**, 8302 (1987).
2. N. D. Mermin and H. Wagner, Phys. Rev. Lett. **22**, 1133 (1966).
3. K. Kubo Phys. Rev. Lett. **61**, 110 (1988). K. Kubo and T. Kishi, Phys. Rev. Lett. **61**, 2585 (1988).
4. P. W. Anderson, Phys. Rev. **86**, 694 (1952). R. Kubo, Phys. Rev. **87**, 568 (1952). T. Oguchi, Phys. Rev. **117**, 117 (1960).
5. M. Parrinello and T. Arai, Phys. Rev. **B10**, 265 (1974). D. Huse, Phys. Rev. *B37*, 2380 (1988).
6. J. Oitmaa and D.D. Betts, Can. J. Phys. **56**, 897 (1978). J. D. Reger and A. P. Young, Phys. Rev **B37**, 5978 (1988). S. Miyashita, J. Phys. Soc. Jpn. **57**, 1934 (1988). T. Barnes, Phys. Rev. **B37**, 9405 (1988). Y. Okabe and M. Kicuchi, J. Phys. Soc. Jpn. **57**, 4351 (1988).
7. M. Gross, E. Sànchez-Velasco and E. Siggia, Phys. Rev. **B39**, 2484.
8. J. Carlson, Phys. Rev. **B40**, 846 (1989). N. Trivedi and D. Ceperley, *ibid.* **B40**, 2747 (1989).
9. E. Manousakis, Phys. Rev. **B40**, 4904 (1989).
10. Z. Liu and E. Manousakis, Phys. Rev. **B40**, 11437 (1989).
11. E. Manousakis and R. Salvador, Phys. Rev. Lett. **60**, 840 (1988).
12. E. Manousakis and R. Salvador, Phys. Rev. **B39**, 575 (1989).
13. E. Manousakis and R. Salvador, Phys. Rev. Lett. **62**, 1310 (1989); and Phys. Rev. **B40**, 2205 (1989).
14. F. D. M. Haldane, Phys. Lett. **93 A**, 464 (1983); Phys. Rev. Lett. bf 50, 1153 (1983). T. Dombre and N. Read, Phys. Rev. **B 38**, 7181 (1988); E. Fradkin and M. Stone, *ibid* **38**, 7215 (1988); L. B. Ioffe and A. I. Larkin, Int. J. Mod. Phys. **B 2**, 203 (1988); X.-G. Wen and A. Zee, Phys. Rev. Lett. **61**, 1025 (1988), F.D.M. Haldane, *ibid* **61**, 1029 (1988).
15. D. Vaknin, S.K.Sinha, D.E. Moncton, D.C. Johnston, J.M. Newsam, C.R. Safinya and H.E. King, Jr. Phys. Rev. Lett. **58**, 2802 (1987). G. Shirane, Y. Endoh, R.J.Birgeneau, M. A. Kastner, Y. Hidaka, M. Oda, M. Suzuki, and T. Murakami, Phys. Rev. Lett. **59**, 1613 (1987). Y. Endoh, et al., Phys. Rev., **B37**, 7443 (1988). K. Yamada, K. Kakurai, Y. Endoh, T. R. Thurston, M. A. Kastner, R. J. Birgeneau. G. Shirane, Y. Hidaka and T. Murakami, Preprint.
16. S. Chakravarty, B.I. Halperin, and D. Nelson, Phys. Rev. Lett. **60**, 1057 (1988).
17. S. Chakravarty, B.I. Halperin, and D. Nelson, Phys. Rev. **B39**, 2344 (1989).
18. M. Boninsegni and E. Manousakis, to be published. See also *Quantum Simulations of Condensed Matter Phenomena*, Los Alamos, NM, August 8-11, 1989, (World Scientific).
19. E. Kaxiras and E. Manousakis, Phys. Rev. **B38**, 866 (1988) and Phys. Rev. **B37**, 656 (1988).
20. L. Hulthen, Ark. Mat. Astr. Fys., **26A**, No. 1 (1938). P. W. Kastelijn, Physica **18**, 104 (1952). W. Marshall, Proc. R. Soc. London, Ser. A **232**, 48 (1955). R. Bartkowski, Phys. Rev. **B5**, 4536 (1972).

21. D. A. Huse and V. Elser, Phys. Rev. Lett. **60**, 2531 (1988). P. Horsch and W. von der Linden: Z. Phys. **B72**, 181 (1988).
22. G. V. Chester and L. Reatto, Phys. Lett. **22**, 276 (1966).
23. H. Neuberger, T. Ziman, Phys. Rev. **B39**, 2608 (1989). M. Gross, E. Sánchez-Velasco and E. Siggia, Phys. Rev. **B39**, 2484 (1989).
24. R. R. P. Singh, P. A. Fleury, K. B. Lyons, P. E. Sulewski, Phys. Rev. Lett. **62**, 2736 (1989).
25. M. Gross, E. Sánchez-Velasco and E. Siggia, Preprint.
26. D. P. Arovas and A. Auerbach, Phys. Rev. **B38**, 316 (1988). M. Takahashi, Phys. Rev. **B40**, 2494 (1989),
27. E. Brèzin, J. Physique, **43**, 15 (1982).
28. K. B. Lyons, P.A. Fleury, J.P.Remeika and T.J. Nergan, Phys. Rev. **B37**, 2353 (1988).
29. G. Aeppli, et al., Phys. Rev. Lett. **62**, 2052 (1989).
30. R. P. Feynman and M. Cohen, Phys. Rev. **102**, 1189 (1957).
31. E.Dagotto, A.Moreo, R.Joynt, S.Bacci, and E. Gagliano, NSF-ITP-89-74, May, 1989. C. -X. Chen and H.-B. Schüttler, Univ. of Georgia, Preprint, 1989.
32. B.Shraiman and E.Siggia, Phys. Rev. Lett. **60**, 740 (1988). C.Gros and M.D.Johnson, to be published. C.L.Kane, P.A. Lee, and N.Read, Phys. Rev. **B39**, 6880 (1989). S. Schmitt-Rink, C. M. Varma, and A. E. Ruckenstein, Phys. Rev. Lett. **60**, 2793 (1988).
33. N. Bulut, D. Hone, E. Loh and D. Scalapino, Phys. Rev. Lett. **62**, 2192 (1989).
34. J. R. Schrieffer, X. -G. Wen and S. -C. Zhang, Phys. Rev. Lett. **60**, 944 (1988).